Sensors and Actuators B 177 (2013) 1134–1141

Contents lists available at SciVerse ScienceDirect

Sensors and Actuators B: Chemical

journal homepage: www.elsevier.com/locate/snb

$ZnO/Al_2O_3/CeO_2$ composite with enhanced gas sensing performance

Qing-Hong Xu [a], Dong-Mei Xu [a], Mei-Yu Guan [a], Ying Guo [a,*], Qi Qi [b], Guo-Dong Li [b,**]

[a] State Key Laboratory of Chemical Resource Engineering, Beijing University of Chemical Technology, P.O. Box 98, Beijing 100029, PR China
[b] State Key Laboratory of Inorganic Synthesis & Preparative Chemistry, College of Chemistry, Jilin University, 2699 Qianjin Street, Changchun 130012, PR China

ARTICLE INFO

Article history:
Received 25 September 2012
Received in revised form 2 December 2012
Accepted 6 December 2012
Available online xxx

Keywords:
Layered double hydroxides
Composite oxides
Gas sensing
Ethanol

ABSTRACT

In this paper, two kinds of layered double hydroxides (LDHs), ZnAl LDH and Ce-doped ZnAl LDH, were introduced as precursors to prepare composite oxides for gas sensing studies. Compared with ZnO/Al_2O_3 based from ZnAl LDH, the $ZnO/Al_2O_3/CeO_2$ composite oxide obtained from Ce-doped ZnAl LDH shows higher gas response to ethanol and shorter response/recovery time as well as remarkable selectivity. The structure, morphology and chemical composition of the gas sensing materials were characterized by X-ray diffraction (XRD), scanning electron microscopy (SEM), high-resolution transmission electron microscopy (HRTEM) and element analysis studies. Raman spectroscopy and X-ray photoelectron spectroscopy (XPS) were used to examine the microstructure and chemical state of the composite oxides sensing materials.

1. Introduction

Gas sensors are very important in many fields, such as industrial emission, household security, vehicle emission control, environmental monitoring, and food nutrition and safety [1–3]. Among them, ethanol sensors have attracted great attention due to their applications in biomedical, chemical and food industries [4,5], particularly the need for the detection of alcohol on human breath to prevent drunk driving or the leaks in industrial distribution lines to avoid loss [6,7]. Furthermore, since ethanol could serve as a non-toxic organic solvent and has recently been found to play a crucial role as an alternative to automotive fuels, the research focused on ethanol monitoring has became more and more important.

Semiconducting metal oxides, for instance ZnO [8], SnO_2 [4], TiO_2 [9], In_2O_3 [10], Fe_2O_3 [11], V_2O_5 [12], WO_3 [13], CeO_2 [14] etc., have shown considerable impact in gas detection due to their low cost and flexibility in production, simplicity in use, large number of detectable gases and various application fields [15]. However, few of them are suitable to all requirements of gas sensors with high sensitivity, short response and recovery time, low detection limit, good selectivity and long-term stability. For this situation, more recent researches have been focusing on composite materials, for example $ZnO–CeO_2$ [16], $ZnO–SnO_2$ [17] and $CeO_2–Fe_2O_3$ [18,19] etc. Comparing sensors with one component, sensors based on two or more components may have the enhanced gas sensing performance from two aspects: a synergistic effect and/or a heterojunction interaction between these components [20].

Undoubtedly, using layered double hydroxides (LDHs) as precursors and then via a calcined process is an alternative way to prepare composite oxides with desired chemical composition and homogeneous elements distribution. LDHs are synthetic two-dimensional nanostructured anionic clays which have a general formula $[M(II)_{1-x}M'(III)_x(OH)_2](A^{n-})_x \cdot yH_2O$ (M(II) = Zn, Mg, Fe, Co, Ni, etc.; M′(III) = Al, Fe, Cr, Co, Ga, In; $A = CO_3^{2-}$, NO_3^-, Cl^-, etc.) [21]. Moreover, some metals ions with M(IV) [22] oxidation states also have the opportunity to form LDHs by partial or even completely replacing M′(III). Since the kinds of metal cations and their proportions can be changed under certain conditions, up to now, more and more composite oxides based on LDH precursors have been prepared successfully and used widely as catalysts or catalyst supports [23], electrode materials [24], magnetic materials [25], etc.

However, to the best of our knowledge, there are only few reports [26] using LDHs as precursors to prepare composite oxides for gas detection applications. As the composite oxides obtained from LDHs precursors have always shown high distribution of metal elements, small crystallite size and high stability against sintering [27], it would have a promising application in gas sensing field if using LDH precursors to prepare composite oxides. Herein, we prepared composite oxides ZnO/Al_2O_3 and $ZnO/Al_2O_3/CeO_2$ for gas sensing studies by taking the ZnAl layered double hydroxide (ZnAl LDH) and Ce-doped ZnAl layered double hydroxide (Ce-doped ZnAl LDH) as the precursors, respectively. Gas sensing measurements have shown that both composite oxides are sensitive in ethanol detection, in particular $ZnO/Al_2O_3/CeO_2$ presents a much higher response and shortened response/recovery times to ethanol

* Corresponding author. Tel.: +86 10 64412115.
** Corresponding author. Tel.: +86 431 85168318.
E-mail addresses: guoying@mail.buct.edu.cn, guoyingbuct@gmail.com (Y. Guo), lgd@jlu.edu.cn (G.-D. Li).

0925-4005/$ – see front matter © 2012 Elsevier B.V. All rights reserved.
http://dx.doi.org/10.1016/j.snb.2012.12.029

than ZnO/Al_2O_3 has, which indicates that the doping of Ce in the ZnAl LDH precursor plays an important effect on improving the gas sensing behaviors. Furthermore, $ZnO/Al_2O_3/CeO_2$ also exhibits superior gas sensing properties to $ZnO/Al_2O_3/CeO_2$-mix obtained from the calcination of mixed metallic salts, which indicates that the approach using LDH as the precursor is a feasible and facile way to prepare composite oxides with better gas sensing performance than that obtained from traditional calcination of mixed metallic salts.

2. Experimental

2.1. Preparation of ZnAl LDH and Ce-doped ZnAl LDH

The starting materials were $Zn(NO_3)_2{\cdot}6H_2O$ (99.0% purity from Xilong Chemical Co., Ltd), $Al(NO_3)_3{\cdot}9H_2O$ (99.0% purity from Xilong Chemical Co., Ltd), $Ce(SO_4)_2{\cdot}4H_2O$ (80.0% purity from Beijing chemical plant) and NaOH (96.0% purity from Beijing chemical plant).

The precursor ZnAl LDH was prepared following a classical co-precipitation method. A solution of NaOH (2 M) was added drop wise over 30 min to a solution (50 ml) containing $Zn(NO_3)_2{\cdot}6H_2O$ (2.97 g, 0.01 mol) and $Al(NO_3)_3{\cdot}9H_2O$ (1.50 g, 0.005 mol) with vigorous stirring. The pH value of the solution at the end of addition was 8.0. The resultant precipitate was maintained at 80 °C and kept stirring for 48 h, centrifuged and washed thoroughly with water before being dried at 60 °C for 24 h.

The Ce-doped ZnAl LDH was prepared using a modified procedure based on previous reports [22,28], which is similar to the preparation of ZnAl LDH that using 0.004 mol $Al(NO_3)_3{\cdot}9H_2O$ and 0.001 mol $Ce(SO_4)_2{\cdot}4H_2O$ instead of 0.005 mol $Al(NO_3)_3{\cdot}9H_2O$.

2.2. Preparation of composite oxides for gas sensing

For the thermal treatment, ZnAl LDH was placed in a muffle furnace and then was calcined at 600 °C for 5 h. After that, the product obtained was named as ZnO/Al_2O_3. Ce-doped ZnAl LDH was heated under the same condition for ZnAl LDH and the obtained gas sensing material was named as $ZnO/Al_2O_3/CeO_2$.

For comparison, the three salts of $Zn(NO_3)_2{\cdot}6H_2O$, $Al(NO_3)_3{\cdot}9H_2O$ and $Ce(SO_4)_2{\cdot}4H_2O$ were mixed up with the same stoichimetric ratio of metallic elements in $ZnO/Al_2O_3/CeO_2$ by physical blending and then were calcined under the above condition to prepare composite oxide, which was named as $ZnO/Al_2O_3/CeO_2$-mix.

2.3. Characterization

Elemental analysis of the precursors was performed with a Shimadzu ICPS-7500 inductively coupled plasma emission spectrometer (ICPES). X-ray diffraction (XRD) measurement was performed on a Rigaku XRD-6000 diffractometer, using Cu Kα radiation (λ = 1.5418 Å) at 40 kV and 30 mA. Scanning electron microscopy (SEM) images were obtained using a Zeiss SUPRA 55 at 20 kV, with the surface of the samples coated with a thin platinum layer to avoid a charging effect. High-resolution transmission electron microscope (HRTEM) was recorded on a JEOL J-2100 to examine the morphologies, lattice fringes and crystal boundaries of the samples. Raman spectroscopy was recorded on a LabRM Aramis Raman instrument using the line of 532 nm laser at the room temperature. Surface elemental analysis was performed using Thereto VGESCALAB 250 X-ray photoelectron spectroscopy (XPS). The binding energy was corrected by contaminant carbon (C 1s = 284.6 eV) in order to facilitate the comparisons of the values among the different gas sensing materials. Peak fitting is done using XPSEAK 4.1, with Shirley background and 70% Lorentz–Gaussian convolution product shapes.

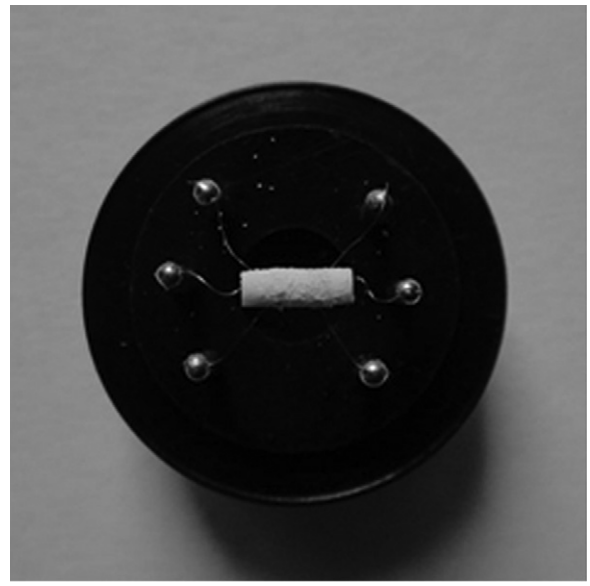

Fig. 1. A photograph of the gas sensor of $ZnO/Al_2O_3/CeO_2$.

2.4. Gas sensing measurements

The test was conducted in a measuring system of chemical gas sensing-8 (CGS-8) in ELITE TECH. In a similar fabrication way to Xu's [8], the composite oxide material was ground in an agate mortar with a little water to form a paste. The paste was coated onto an alumina ceramic tube attached with a pair of Pt electrodes for resistance measurement. A small Ni–Cr alloy coil was placed through the tube as a heater, which provides the working temperature of the gas sensor by varying the heating current. Fig. 1 presents a photograph of the gas sensor of $ZnO/Al_2O_3/CeO_2$.

The gas response was designated as R_a/R_g, where R_a was the sensor resistance in air (base resistance) and R_g was that in the target gas. The time taken by the sensor resistance to change from R_a to $R_a - 90\% \times (R_a - R_g)$ was defined as response time after the target gas was introduced to the sensor, and the time taken from R_g to $R_g + 90\% \times (R_a - R_g)$ was defined as recovery time after the ambience was replaced by air.

3. Results and discussion

3.1. Structure, morphologies and gas sensing characterization

Fig. 2A shows the XRD patterns of ZnAl LDH and Ce-doped ZnAl LDH. The (0 0 3), (0 0 6), (0 0 9) and (1 1 0) diffraction peaks, which correspond to the basal and higher order reflections, appear at 10.08°, 20.10°, 30.14°, 60.37°, respectively. Apparently, the XRD pattern for ZnAl LDH exhibits the characteristic reflections of LDH materials with (0 0 *l*) peaks, which are evidences for the layered structure [29]. Compared with ZnAl LDH, the strength of diffraction peaks reduce significantly for Ce-doped ZnAl LDH. It is probably difficult for Ce^{4+} to replace Al^{3+} staying in the host layer of LDH since the radius of Ce^{4+} is much larger than Al^{3+}, which leads to the decrease of the crystallinity. Fortunately, the positions of diffraction peaks for Ce-doped ZnAl LDH nearly stay the same as ZnAl LDH, which indicates that the structure of Ce-doped ZnAl LDH has remained the layered structure and no new impure phase appears. Moreover, according to the element analyses (Table S1), the content percent of Ce is 6.14% in Ce-doped ZnAl LDH.

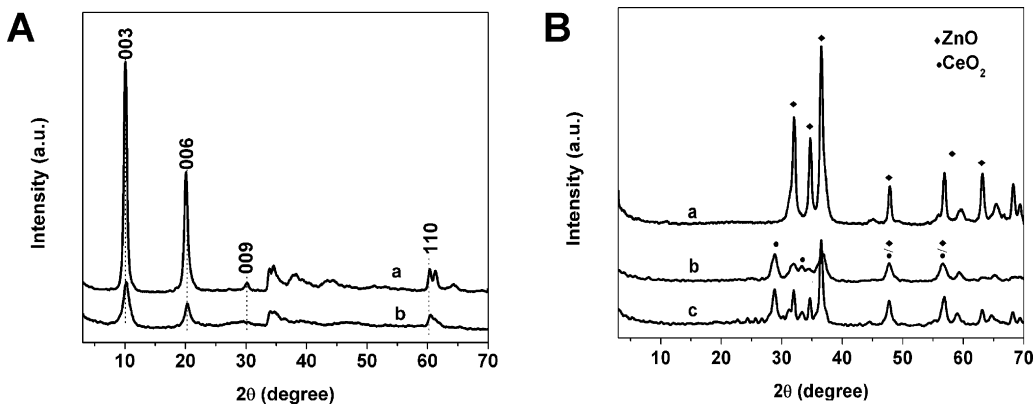

Fig. 2. X-ray diffraction patterns of LDH precursors (A: a – ZnAl-LDH and b – Ce-doped ZnAl LDH) and the calcined LDHs (B: a – ZnO/Al_2O_3, b – $ZnO/Al_2O_3/CeO_2$ and c – $ZnO/Al_2O_3/CeO_2$-mix).

Fig. 2B shows the XRD for the calcined products of ZnO/Al_2O_3, $ZnO/Al_2O_3/CeO_2$ and $ZnO/Al_2O_3/CeO_2$-mix. As shown in Fig. 2B, the most conspicuous peaks for the calcined ZnAl LDH, ZnO/Al_2O_3, show the presence of diffractions of hexagonal ZnO phase at 31.86° (1 0 0), 34.52° (0 0 2), 36.34° (1 0 1), 47.64° (1 1 2) and 56.74° (1 1 0). It means that the composite oxide based on ZnO was prepared successfully with a high degree of crystallization. While for $ZnO/Al_2O_3/CeO_2$ and $ZnO/Al_2O_3/CeO_2$-mix, their XRD patterns not only show the characteristic peaks for ZnO, but also show the presence of the characteristic diffraction peaks of cubic CeO_2 phase, such as the peaks at 28.55° (1 1 1), 33.27° (2 2 0), 47.48° (2 2 0) and 56.33° (3 1 1). The diffraction peaks of (2 2 0) and (3 3 1) of CeO_2 are superposed on the diffraction peaks of (1 1 2) and (1 1 0) of ZnO. No significant diffractions of Al_2O_3 are observed in the three composite oxides.

The morphologies and microstructures of the obtained composite metal oxides were characterized by SEM and HRTEM. From Fig. 3A several sheets constructed by a number of small particles are clearly observed, which indicates that the oxides were obtained by sacrificing the template of LDHs. As shown in Fig. 3B, these particles mainly present well-crystallized hexagonal crystals with high degree of order. Moreover, as shown in HRTEM images (Fig. 3C), these hexagonal crystals are proved to be the phase of ZnO as the spacing between adjacent lattice planes is 0.24 nm which is corresponding to the (1 0 1) planes of wurtzite ZnO. It is clear that the size of ZnO is in a range of 5–60 nm. For the composite oxide obtained from Ce-doped ZnAl LDH, many irregular particles are obviously observed as in the SEM image (Fig. 3D) while the sheets of their precursor are small and not obvious. In the images of HRTEM (Fig. 3E and F), both CeO_2 and ZnO are close to spherical in shape with a homogeneous size at about 10 nm and the interplanar spacing of CeO_2 (1 1 1) and ZnO (0 0 2) can be easily distinguished. Compared with the $ZnO/Al_2O_3/CeO_2$, $ZnO/Al_2O_3/CeO_2$-mix shows irregular morphology and undistinguished boundary in the SEM (Fig. 3G) and HRTEM (Fig. 3H). It is very difficult to determine the shape and size of $ZnO/Al_2O_3/CeO_2$-mix in Fig. 3H. Only from the amplified image (Fig. 3I), the fringe lattice image belongs to ZnO and CeO_2 could be obviously discerned. That is to say, the composite oxide obtained from physical mixed salts is aggregated and probably in a heterogeneous distribution.

3.2. Raman spectroscopy

Raman spectroscopy was also further employed to study the microstructures of the three composite oxides materials. All of the spectra were collected by at least ten times scanning at different regions. Fig. 4a and b are the Raman spectra of ZnO/Al_2O_3 and $ZnO/Al_2O_3/CeO_2$, respectively. However, the product obtained from the physical mixed salts presents diverse spectra in Fig. 4c and d, which are the spectra we collected from different regions of $ZnO/Al_2O_3/CeO_2$-mix. It further indicates that the metallic elements in the composite oxides obtained from LDHs are in a uniform distribution, whereas those obtained from the mixed salts are not, which is in accordance with the SEM and HRTEM images. As shown in Fig. 4a, the ZnO powder phase in ZnO/Al_2O_3 is easily detected by the well-defined Raman scattering bands at 435 cm^{-1} and 578 cm^{-1}. The band at 435 cm^{-1} can be attributed to the E_2 (high) mode for the wurtize hexagonal phase of ZnO [30,31]. The suppressed band at 578 cm^{-1} can be attributed to the E_1 (longitudinal optical, LO) mode, which indicates a high crystalline quality and low oxygen vacancy for ZnO [31]. Compared with ZnO/Al_2O_3, the spectrum of $ZnO/Al_2O_3/CeO_2$ exhibits some new bands at ~460, ~600, ~993 and ~1041 cm^{-1}. The dominated and strong band at 460 cm^{-1} corresponds to F_{2g} vibration of CeO_2 cubic lattice [32]. The presence of a weak and less prominent broad band near 600 cm^{-1} could be attributed to a doubly degenerate LO of CeO_2. Normally, this band has been linked to oxygen vacancies in the CeO_2 lattice [33]. The Raman band at 993 and 1041 cm^{-1} can be assigned to the stretching vibration band of SO_4^{2-} [34,35], which indicates that a small quantity of sulfates during the synthesis of Ce-doped ZnAl LDH still remained even after calcination.

3.3. X-ray photoelectron spectroscopy

The samples of $ZnO/Al_2O_3/CeO_2$ and $ZnO/Al_2O_3/CeO_2$-mix have been investigated by XPS technique. As shown in Fig. S1 and Table S2, the peaks of Zn 2p and Al 2p have no significant chemical shifts for $ZnO/Al_2O_3/CeO_2$ in comparison with $ZnO/Al_2O_3/CeO_2$-mix. XPS studies of CeO_{2-x} and CeO_2 have been reported by several researchers, where Ce $3d_{5/2}$ and Ce $3d_{3/2}$ levels are composed of 10 various states [36,37]. Fig. 5 presents the fitted curves of Ce for $ZnO/Al_2O_3/CeO_2$ and $ZnO/Al_2O_3/CeO_2$-mix, respectively, while we can see these contributed peaks distinctly from Table 1. After the deconvolution of the Ce 3d spectra, the degree of reduction (Ce^{3+} species) can be estimated by the percentage of peak areas for Ce^{3+} in the whole peak areas for Ce^{3+} and Ce^{4+} [32]. As shown in Tables S2 and 1, the peaks of Ce 3d in $ZnO/Al_2O_3/CeO_2$ shift remarkably to low binding energy in comparison with $ZnO/Al_2O_3/CeO_2$-mix, and the two materials nearly present the same reduction behavior of Ce^{3+}.

Fig. 6 shows O 1s spectra of $ZnO/Al_2O_3/CeO_2$ and $ZnO/Al_2O_3/CeO_2$-mix, respectively. The O 1s is fitted with three peaks, referred to as O_I, O_{II}, O_{III} components (Table 2). Component O_I with binding energy ≈ 532.6 ± 0.04 eV is usually attributed

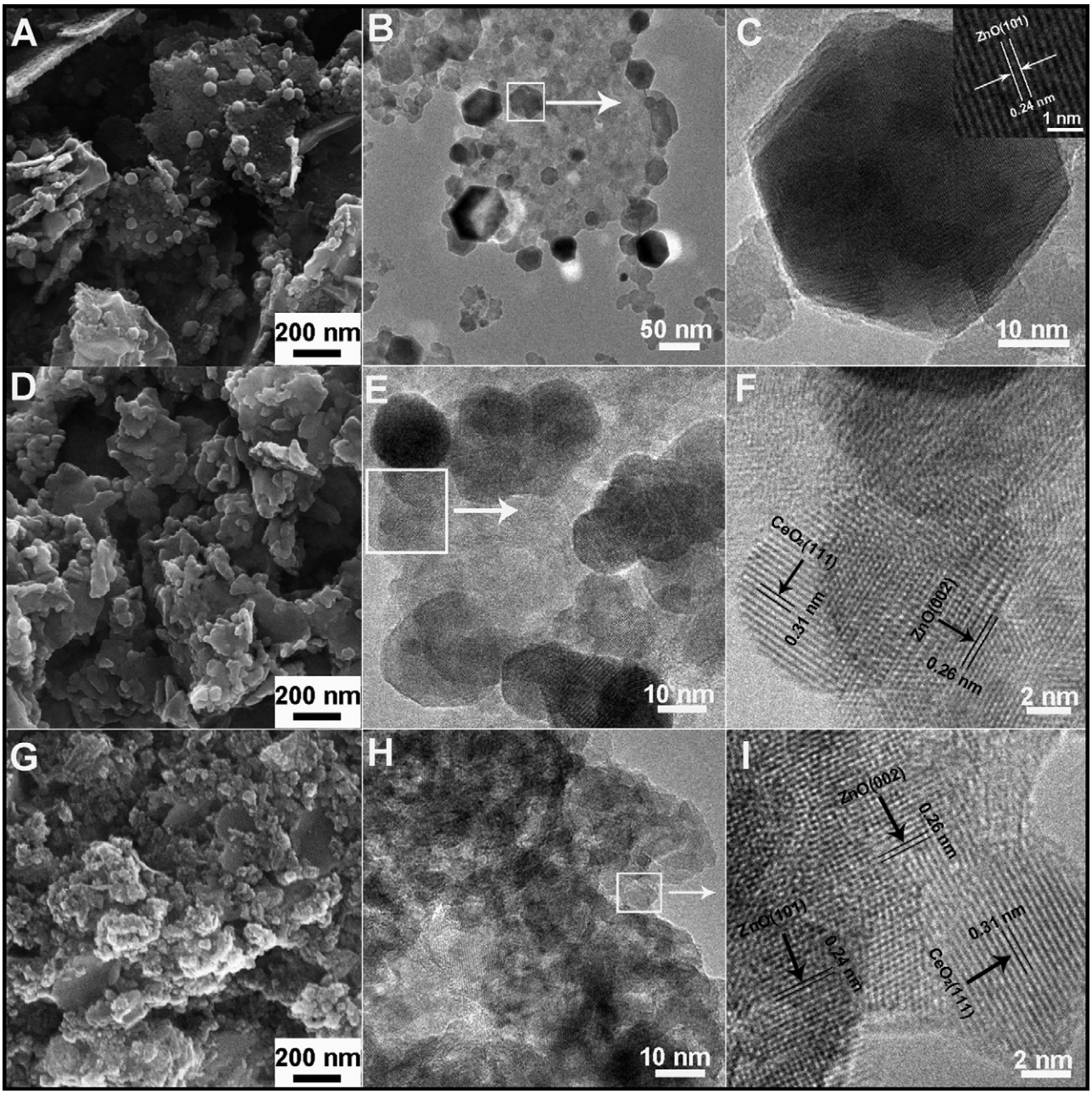

Fig. 3. SEM (A) and HRTEM (B and C) images for ZnO/Al_2O_3, SEM (D) and HRTEM (E and F) images for $ZnO/Al_2O_3/CeO_2$, SEM (G) and HRTEM (H and I) images for $ZnO/Al_2O_3/CeO_2$-mix.

to the presence of loosely bound oxygen on the surface of the composite oxide belonging to a specific species, e.g. adsorbed H_2O or adsorbed O_2 [38]. Component O_{III} with the lowest binding energy near 530 eV belongs to the lattice oxygen in composite oxide [36,38,39]. The medium binding energy component O_{II} centered at 531.4 ± 0.05 eV is associated with O^{2-} ions that are in oxygen deficient regions with the matrix of composite oxide [38,39]. Therefore, as the peak area of O_{II} in $ZnO/Al_2O_3/CeO_2$ is accounted for a larger proportion (in Table 2), we can deduce that the oxygen deficiency in the surface is larger in $ZnO/Al_2O_3/CeO_2$ than that in $ZnO/Al_2O_3/CeO_2$-mix.

3.4. Ethanol sensing measurements

The responses to 1000 ppm ethanol of the three composite oxides materials at various temperatures are shown in Fig. 7. All materials exhibit different sensing properties at different operating temperature conditions. As can be seen, the optimal operating

Table 1
Energy positions of the spectral components in Ce 3d observed in $ZnO/Al_2O_3/CeO_2$ and $ZnO/Al_2O_3/CeO_2$-mix.

Samples	Binding energy of Ce^{4+} (eV)						Binding energy of Ce^{3+} (eV)				Ce^{3+} (%)
$ZnO/Al_2O_3/CeO_2$	915.6	906.5	900.4	897.4	887.5	881.6	903.1	899.3	884.9	880.3	26
$ZnO/Al_2O_3/CeO_2$-mix	915.6	907.0	900.4	897.8	887.8	882.1	903.2	898.7	884.9	880.4	29

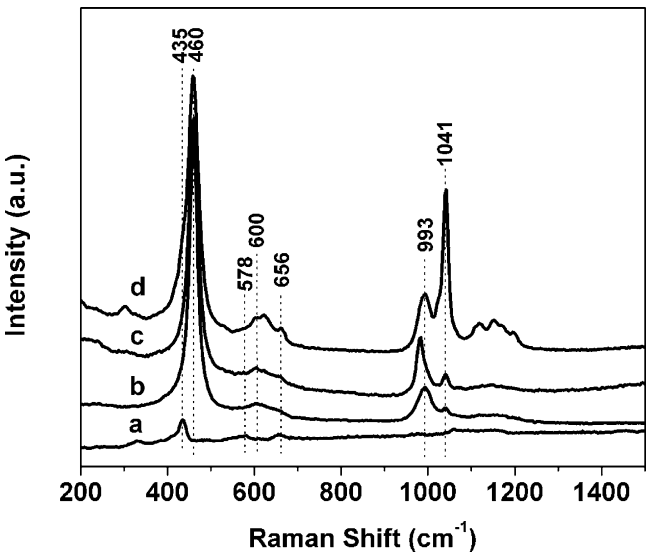

Fig. 4. Raman spectra of ZnO/Al_2O_3 (a), $ZnO/Al_2O_3/CeO_2$ (b) and $ZnO/Al_2O_3/CeO_2$-mix at different region (c and d).

temperatures of $ZnO/Al_2O_3/CeO_2$ and $ZnO/Al_2O_3/CeO_2$-mix for achieving the max ethanol response are obtained at about 260 °C, while the optimal operating temperature of ZnO/Al_2O_3 is 310 °C. The responses are obtained by increasing the operating temperature below every optimal operating temperature, which can be explained by the enhanced activation of the materials. However, the gas sensing response would decline above the optimal operating temperature, which might be contributed to the competing desorption of oxygen [40]. Among the three gas sensing materials, the ethanol response of $ZnO/Al_2O_3/CeO_2$ is the highest in the range of 200–300 °C, while below 200 °C or above 300 °C the ethanol response of $ZnO/Al_2O_3/CeO_2$ is a little lower than $ZnO/Al_2O_3/CeO_2$-mix but still much higher than ZnO/Al_2O_3. At the optimal operating temperature of $ZnO/Al_2O_3/CeO_2$ (260 °C), the ethanol response of $ZnO/Al_2O_3/CeO_2$ reaches 170, which is about 2.4 times of $ZnO/Al_2O_3/CeO_2$-mix and 15.4 times of ZnO/Al_2O_3. Therefore, all the above results indicate that the introduction of Ce plays an important role on the improvement of the ethanol responses and lowering the optimal operating temperatures.

Table 2
Energy positions of the spectral components in O 1s in $ZnO/Al_2O_3/CeO_2$ and $ZnO/Al_2O_3/CeO_2$-mix.

Samples	Binding energy of O 1s (eV)			O_I:O_{II}:O_{III}
	O_I	O_{II}	O_{III}	
$ZnO/Al_2O_3/CeO_2$	532.6	531.4	530.4	0.15:0.64:0.21
$ZnO/Al_2O_3/CeO_2$-mix	532.6	531.5	530.1	0.19:0.49:0.32

Fig. 8 shows the response and recovery time for the three composite oxides materials. The first 50 s show their responses in the air, after that the air was replaced by 1000 ppm ethanol in air and remained as such for 100 s. At 150 s the environment was switched back to air again. As is shown in Table 3, the response and recovery times of $ZnO/Al_2O_3/CeO_2$ to 1000 ppm ethanol at

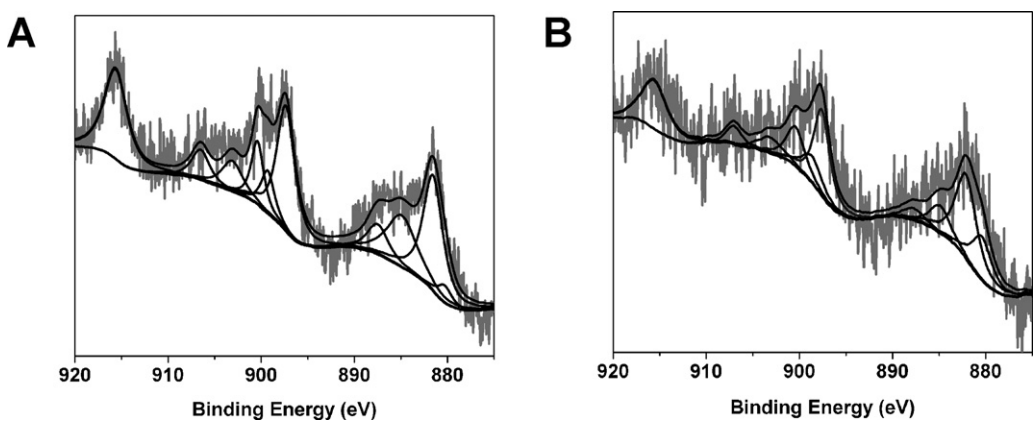

Fig. 5. Ce 3d XP spectra of (A) $ZnO/Al_2O_3/CeO_2$ and (B) $ZnO/Al_2O_3/CeO_2$-mix.

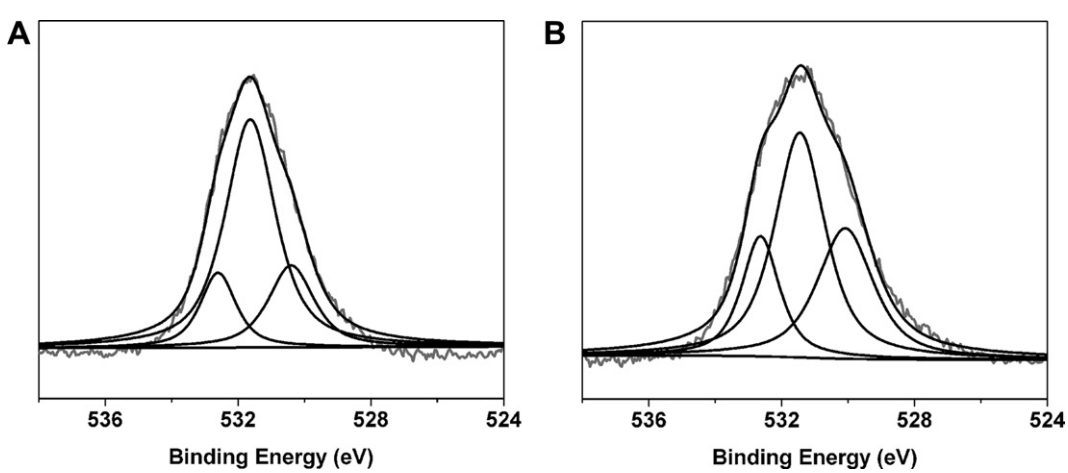

Fig. 6. O 1s XP spectra of (A) $ZnO/Al_2O_3/CeO_2$ and (B) $ZnO/Al_2O_3/CeO_2$-mix.

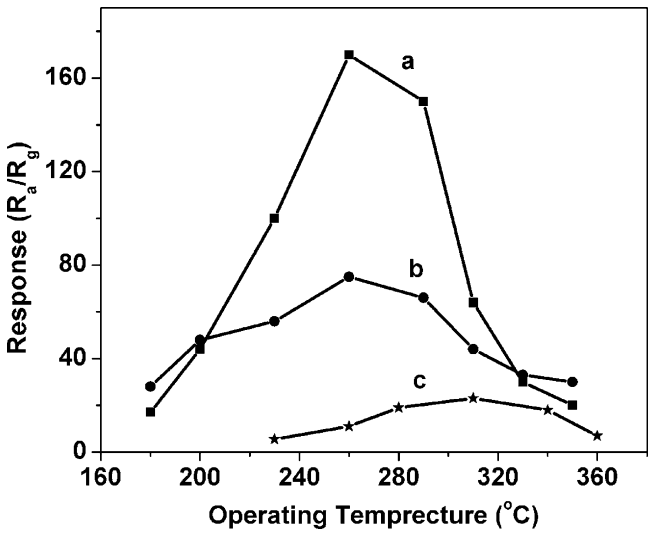

Fig. 7. Responses of gas sensing materials made to 1000 ppm CH_3CH_2OH versus operating temperatures. (a) $ZnO/Al_2O_3/CeO_2$, (b) $ZnO/Al_2O_3/CeO_2$-mix and (c) ZnO/Al_2O_3.

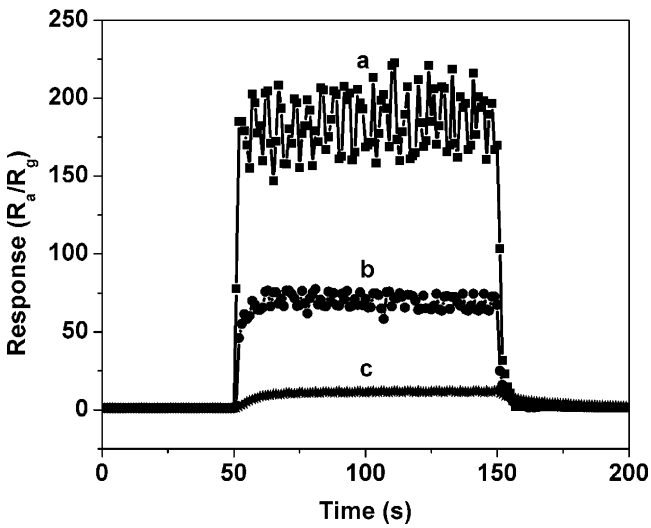

Fig. 8. Response–recovery curves of gas sensing materials made to 1000 ppm CH_3CH_2OH at 260 °C. (a) $ZnO/Al_2O_3/CeO_2$, (b) $ZnO/Al_2O_3/CeO_2$-mix and (c) ZnO/Al_2O_3.

260 °C are about 2 s and 10 s, respectively, which are much shorter than $ZnO/Al_2O_3/CeO_2$-mix and ZnO/Al_2O_3. It further proves that $ZnO/Al_2O_3/CeO_2$ has the best ethanol sensing behavior among the three composite oxides materials.

The $ZnO/Al_2O_3/CeO_2$ was further exposed to different concentrations of ethanol gases at 260 °C and the responses vs. ethanol concentrations are shown in Fig. 9. The material can detect ethanol vapor down to 50 ppm with the gas response value of 30. With the enhancing of ethanol concentration, the responses increase accordingly. The response reaches 250 for $ZnO/Al_2O_3/CeO_2$ to 2000 ppm ethanol.

Table 3
The response and recovery times of the gas sensing materials.

Samples	Response time	Recovery time
ZnO/Al_2O_3	14 s	87 s
$ZnO/Al_2O_3/CeO_2$	2 s	10 s
$ZnO/Al_2O_3/CeO_2$-mix	6 s	85 s

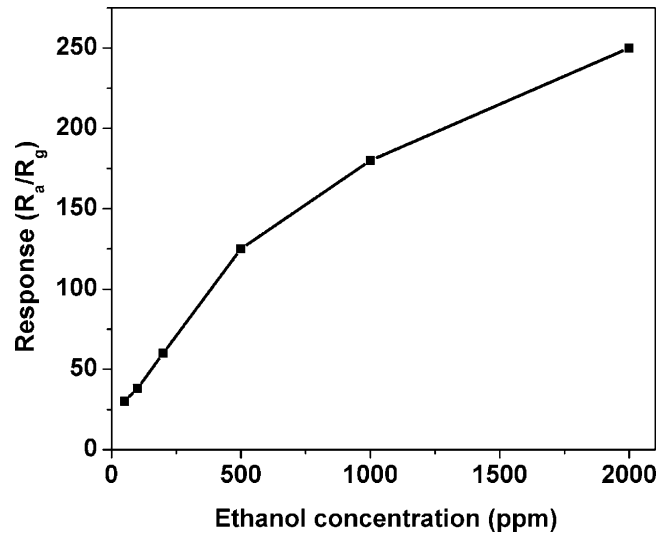

Fig. 9. Responses of $ZnO/Al_2O_3/CeO_2$ versus ethanol concentrations at 260 °C.

In comparison with the previous studies of ZnO or CeO_2-based gas sensing materials which are listed in Table 4 [40–46], the gas sensing performance of $ZnO/Al_2O_3/CeO_2$ to ethanol is comparable as it has a relatively high gas response, low operating temperature and short response/recovery time. Therefore, the further gas selectivity measurements are focused on this sample.

Furthermore, the selectivity of gas sensor is also an important factor for further application. Fig. 10 shows the gas sensing selectivity of $ZnO/Al_2O_3/CeO_2$. It is found that $ZnO/Al_2O_3/CeO_2$ exhibits very high response to ethanol but less response to methanol and very low responses to CO, NH_3, C_7H_8 (toluene), MF (formamide), gasoline with the same concentrations of 1000 ppm, indicating that the $ZnO/Al_2O_3/CeO_2$ at 180–350 °C is a good candidate for highly selective detection of ethanol.

3.5. Gas sensing mechanism

Based on our results, the gas sensing mechanism for these composite oxides ZnO, CeO_2 and Al_2O_3 has been discussed as follows.

It is well known that when the ZnO-based gas sensors are surrounded by air, oxygen molecules are adsorbed on the ZnO surface

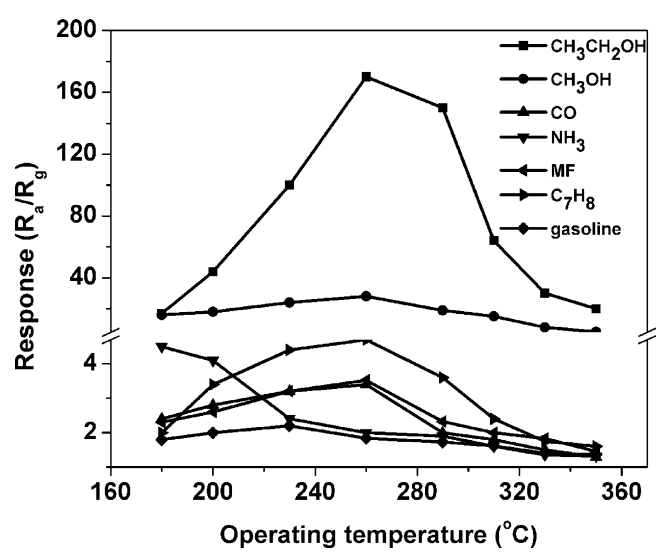

Fig. 10. Responses of $ZnO/Al_2O_3/CeO_2$ to varied gases (1000 ppm) versus operating temperatures.

Table 4
The gas sensing properties of $ZnO/Al_2O_3/CeO_2$ compared with the references based on ZnO or CeO_2.

Gas sensors	Ethanol concentration (ppm)	Response (R_a/R_g)	Operation temperature (°C)	Response/recovery time	References
$ZnO/Al_2O_3/CeO_2$	1000	170	260	2/10 s	Our result
	50	30			
ZnO nanorods	1000	50	332	10/30 s	[43]
ZnO nanorods	1000	293	450	<10 s	[44]
CeO_2 doped ZnO	500	60	350	200 s	[45]
ZnO:Al films	400	20	250	2–4 m	[46]
ZnO nanorods	100	18	350	10/20 s	[47]
Ce doped ZnO	100	80	320	10/5 s	[48]
ZnO films	30	10	Room temperature	28/49 s	[49]

to form chemisorbed oxygen species (O_2^-, O_2^{2-} and O^{2-}) [47]. When the target gases are in contact with the surface of the sensors, a surface reaction reduces the coverage of oxygen ions and releases electrons to the conduction band of the material, which results in an increase in the conductivity of the samples [47].

Based on the fact that the composite oxide containing CeO_2, especially $ZnO/Al_2O_3/CeO_2$ has superior response to ethanol, we conclude that CeO_2 must play an important role in improving the gas sensing properties. Here, electronic sensitization can be applied to explain the gas sensing mechanism of surface CeO_2 [48]. As a strong acceptor for electrons, CeO_2 induces an electron-depleted layer near the interface in the host semiconductor (ZnO/Al_2O_3) [48]. By reacting with a reducing analyte, for example ethanol, CeO_2 is induced releasing the electrons back to the semiconductor. Due to the facile creation and diffusion of oxygen vacancies, especially at the ceria surfaces, cerium has the capability to absorb and release oxygen and then to undergo rapid and repeatable Ce^{4+}/Ce^{3+} redox cycles depending on certain conditions [43]. Therefore, ethanol would extract more oxygen in a faster time from the gas sensing materials containing CeO_2 than the one without CeO_2 [49], which can be used to explain the higher response and shorter response/recovery time for CeO_2 containing composite oxides. In conclusion, the doping with CeO_2 is in favor of enhancing the gas sensing properties by making possible cooperating effect with ZnO/Al_2O_3.

Simultaneously, Al_2O_3 is a typical dopant with porous structures and it may play a role of "diluent", which can separate crystallites of semiconductor oxides [50].

Moreover, using Ce-doped ZnAl-LDH as precursor to prepare composite of $ZnO/Al_2O_3/CeO_2$, we could obtain homogeneously dispersed metal oxides as shown in SEM, HRTEM and Raman spectra. Compared with $ZnO/Al_2O_3/CeO_2$-mix obtained from mixed salts, the well dispersed composite oxide of $ZnO/Al_2O_3/CeO_2$ might possess strong interaction between ZnO, Al_2O_3 and CeO_2, which accounts for the improved gas response and the shortened response/recovery time.

4. Conclusions

The well dispersed composite metal oxides were successfully synthesized using LDHs as precursors for gas sensing studies. For comparison, the composite $ZnO/Al_2O_3/CeO_2$ obtained from the Ce-doped ZnAl LDH presents excellent gas sensing properties in ethanol detection than that without doping. Moreover, $ZnO/Al_2O_3/CeO_2$ exhibits much higher gas response value and shorter response/recovery time (2 s/10 s to 1000 ppm at 260 °C) than $ZnO/Al_2O_3/CeO_2$-mix prepared from physical mixed salts. The gas response of $ZnO/Al_2O_3/CeO_2$ is 15.4 times higher than that of ZnO/Al_2O_3 and 2.4 times higher than $ZnO/Al_2O_3/CeO_2$-mix to 1000 ppm ethanol at 260 °C, respectively. In conclusion, LDHs have shown good performance to prepare composite oxides for gas sensing applications, especially when introducing Ce as the dopant, of which the obtained product $ZnO/Al_2O_3/CeO_2$ can be used as a good candidate for the detection of ethanol in future use. Furthermore, as the kinds and proportions of metal ions are changeable under certain conditions in LDHs, it may provide us an alternative way to design various composite oxides for gas sensing applications by the calcination of LDHs.

Acknowledgments

This work was supported by the National Natural Science Foundation of China (21001014), Beijing Natural Science Foundation (2113049) and Fundamental Research funds for the Central Universities (QN0908). We thank Beijing Elite Tech Co. Ltd., China, for gas sensing measurements.

Appendix A. Supplementary data

Supplementary data associated with this article can be found, in the online version, at http://dx.doi.org/10.1016/j.snb.2012.12.029.

References

[1] G. Jimenez-Cadena, J. Riu, F.X. Rius, Gas sensors based on nanostructured materials, Analyst 132 (2007) 1083–1099.
[2] A. Tricoli, M. Righettoni, A. Teleki, Semiconductor gas sensors: dry synthesis and application, Angewandte Chemie International Edition 49 (2010) 7632–7659.
[3] E. Comini, Metal oxide nano-crystals for gas sensing, Analytica Chimica Acta 568 (2006) 28–40.
[4] H.-C. Chiu, C.-S. Yeh, Hydrothermal synthesis of SnO_2 nanoparticles and their gas-sensing of alcohol, Journal of Physical Chemistry C 111 (2007) 7256–7259.
[5] X. Song, L. Gao, S. Mathur, Synthesis, characterization and gas sensing properties of porous nickel oxide nanotubes, Journal of Physical Chemistry C 115 (2011) 21730–21735.
[6] S. Tsang, C. Bulpitt, Rare earth oxide sensors for ethanol analysis, Sensors and Actuators B: Chemical 52 (1998) 226–235.
[7] X. Lou, S. Liu, D. Shi, W. Chu, Ethanol-sensing characteristics of $CdFe_2O_4$ sensor prepared by sol–gel method, Materials Chemistry and Physics 105 (2007) 67–70.
[8] J. Xu, J. Han, Y. Zhang, Y. Sun, B. Xie, Studies on alcohol sensing mechanism of ZnO based gas sensors, Sensors and Actuators B: Chemical 132 (2008) 334–339.
[9] P. Hu, G. Du, W. Zhou, J. Cui, J. Lin, H. Liu, D. Liu, J. Wang, S. Chen, Enhancement of ethanol vapor sensing of TiO_2 nanobelts by surface engineering, ACS Applied Materials & Interfaces 2 (2010) 3263–3269.
[10] X. Lai, D. Wang, N. Han, J. Du, J. Li, C. Xing, Y. Chen, X. Li, Ordered arrays of bead-chain-like In_2O_3 nanorods and their enhanced sensing performance for formaldehyde, Chemistry of Materials 22 (2010) 3033–3042.
[11] L. Wang, T. Fei, Z. Lou, T. Zhang, Three-dimensional hierarchical flowerlike α-Fe_2O_3 nanostructures: synthesis and ethanol-sensing properties, ACS Applied Materials & Interfaces 3 (2011) 4689–4694.
[12] J. Liu, X. Wang, Q. Peng, Y. Li, Vanadium pentoxide nanobelts: highly selective and stable ethanol sensor materials, Advanced Materials 17 (2005) 764–767.
[13] A. Labidi, C. Lambert-Mauriat, C. Jacolin, M. Bendahan, M. Maaref, K. Aguir, dc and ac characterizations of WO_3 sensors under ethanol vapors, Sensors and Actuators B: Chemical 119 (2006) 374–379.
[14] H. Imagawa, A. Suda, K. Yamamura, S. Sun, Monodisperse CeO_2 nanoparticles and their oxygen storage and release properties, Journal of Physical Chemistry C 115 (2011) 1740–1745.
[15] G. Korotcenkov, Metal oxides for solid-state gas sensors: what determines our choice? Materials Science and Engineering B 139 (2007) 1–23.
[16] M.F. Al-Kuhaili, S.M.A. Durrani, I.A. Bakhtiari, Carbon monoxide gas-sensing properties of CeO_2–ZnO thin films, Applied Surface Science 255 (2008) 3033–3039.
[17] K.-W. Kim, P.-S. Cho, S.-J. Kim, J.-H. Lee, C.-Y. Kang, J.-S. Kim, S.-J. Yoon, The selective detection of C_2H_5OH using SnO_2–ZnO thin film gas sensors prepared

by combinatorial solution deposition, Sensors and Actuators B: Chemical 123 (2007) 318–324.
[18] G. Neri, A. Bonavita, G. Rizzo, S. Galvagno, S. Capone, P. Siciliano, A study of the catalytic activity and sensitivity to different alcohols of CeO_2–Fe_2O_3 thin films, Sensors and Actuators B: Chemical 111–112 (2005) 78–83.
[19] G. Neri, A. Bonavita, G. Rizzo, S. Galvagno, S. Capone, P. Siciliano, Methanol gas-sensing properties of CeO_2–Fe_2O_3 thin films, Sensors and Actuators B: Chemical 114 (2006) 687–695.
[20] C. Wang, L. Yin, L. Zhang, D. Xiang, R. Gao, Metal oxide gas sensors: sensitivity and influencing factors, Sensors 10 (2010) 2088–2106.
[21] J. Liu, X. Huang, Y. Li, K.M. Sulieman, X. He, F. Sun, Facile and large-scale production of ZnO/Zn–Al layered double hydroxide hierarchical heterostructures, Journal of Physical Chemistry B 110 (2006) 21865–21872.
[22] C.G. Silva, Y. Bouizi, V. Fornes, H. Garcia, Layered double hydroxides as highly efficient photocatalysts for visible light oxygen generation from water, Journal of the American Chemical Society 131 (2009) 13833–13839.
[23] X. Xiang, H.I. Hima, H. Wang, F. Li, Facile synthesis and catalytic properties of nickel-based mixed-metal oxides with mesopore networks from a novel hybrid composite precursor, Chemistry of Materials 20 (2008) 1173–1182.
[24] M. Latorre-Sanchez, P. Atienzar, G. Abellán, M. Puche, V. Fornés, A. Ribera, et al., The synthesis of a hybrid graphene–nickel/manganese mixed oxide and its performance in lithium-ion batteries, Carbon 50 (2012) 518–525.
[25] X. Zhao, Y. Zhang, S. Xu, X. Lei, F. Zhang, Oriented $CoFe_2O_4$/CoO nanocomposite films from layered double hydroxide precursor films by calcination: ferromagnetic nanoparticles embedded in an antiferromagnetic matrix for beating the superparamagnetic limit, Journal of Physical Chemistry C 116 (2012) 5288–5294.
[26] S. Morandi, F. Prinetto, M. Di Martino, G. Ghiotti, O. Lorret, D. Tichit, C. Malagù, B. Vendemiati, M.C. Carotta, Synthesis and characterisation of gas sensor materials obtained from Pt/Zn/Al layered double hydroxides, Sensors and Actuators B: Chemical 118 (2006) 215–220.
[27] L. Zhang, F. Li, D.G. Evans, X. Duan, Structure and surface characteristics of Cu-based composite metal oxides derived from layered double hydroxides, Materials Chemistry and Physics 87 (2004) 402–410.
[28] Y. Wang, W. Peng, L. Liu, F. Gao, M. Li, The electrochemical determination of L-cysteine at a Ce-doped Mg–Al layered double hydroxide modified glassy carbon electrode, Electrochimica Acta 70 (2012) 193–198.
[29] M. Wei, X. Tian, J. He, M. Pu, G. Rao, H. Yang, L. Yang, T. Liu, D.G. Evans, X. Duan, Study of the in situ postintercalative polymerization of metanilic anions intercalated in NiAl-layered double hydroxides under a nitrogen atmosphere, European Journal of Inorganic Chemistry 2006 (2006) 3442–3450.
[30] Z. Zhang, B. Huang, Y. Yu, D. Cui, Electrical properties and Raman spectra of undoped and Al-doped ZnO thin films by metalorganic vapor phase epitaxy, Materials Science and Engineering B 86 (2001) 109–112.
[31] H.-M. Cheng, Hsu, Y.-K. Tseng, L.-J. Lin, W.-F. Hsieh, Raman scattering and efficient UV photoluminescence from well-aligned ZnO nanowires epitaxially grown on GaN buffer layer, Journal of Physical Chemistry B 109 (2005) 8749–8754.
[32] M.S.P. Francisco, V.R. Mastelaro, P.A.P. Nascente, A.O. Florentino, Activity and characterization by XPS, HR-TEM, Raman spectroscopy, and BET surface area of CuO/CeO_2–TiO_2 catalysts, Journal of Physical Chemistry B 105 (2001) 10515–10522.
[33] B.M. Reddy, A. Khan, P. Lakshmanan, M. Aouine, S. Loridant, J.-C. Volta, Structural characterization of nanosized CeO_2–SiO_2, CeO_2–TiO_2, and CeO_2–ZrO_2 catalysts by XRD, Raman, and HREM techniques, Journal of Physical Chemistry B 109 (2005) 3355–3363.
[34] D. Uy, K.A. Wiegand, A.E. O'Neill, M.A. Dearth, W.H. Weber, In situ UV Raman study of the NOx trapping and sulfur poisoning behavior of Pt/Ba/γ-Al_2O_3 catalysts, Journal of Physical Chemistry B 106 (2001) 387–394.
[35] Y. Zhang, C.K. Chan, Understanding the hygroscopic properties of supersaturated droplets of metal and ammonium sulfate solutions using Raman spectroscopy, Journal of Physical Chemistry A 106 (2001) 285–292.
[36] Fc. Larachi, J. Pierre, A. Adnot, A. Bernis, Ce 3d XPS study of composite $Ce_xMn_{1-x}O_{2-y}$ wet oxidation catalysts, Applied Surface Science 195 (2002) 236–250.
[37] S. Watanabe, X. Ma, C. Song, Characterization of structural and surface properties of nanocrystalline TiO_2–CeO_2 mixed oxides by XRD, XPS, TPR, and TPD, Journal of Physical Chemistry C 113 (2009) 14249–14257.
[38] M. Chen, X. Wang, Y. Yu, Z. Pei, X. Bai, C. Sun, R. Huang, L. Wen, X-ray photoelectron spectroscopy and auger electron spectroscopy studies of Al-doped ZnO films, Applied Surface Science 158 (2000) 134–140.
[39] K. Ghosh, M. Kumar, H. Wang, T. Maruyama, Y. Ando, Nitrogen-mediated wet-chemical formation of carbon nitride/ZnO heterojunctions for enhanced field emission, Langmuir 26 (2010) 5527–5533.
[40] L. Bie, X. Yan, J. Yin, Y. Duan, Z. Yuan, Nanopillar ZnO gas sensor for hydrogen and ethanol, Sensors and Actuators B: Chemical 126 (2007) 604–608.
[41] J. Xu, Y. Chen, D. Chen, J. Shen, Hydrothermal synthesis and gas sensing characters of ZnO nanorods, Sensors and Actuators B: Chemical 113 (2006) 526–531.
[42] Y. Lv, L. Guo, H. Xu, X. Chu, Gas-sensing properties of well-crystalline ZnO nanorods grown by a simple route, Physica E 36 (2007) 102–105.
[43] N.F. Hamedani, A.R. Mahjoub, A.A. khodadadi, Y. Mortazavi, CeO_2 doped ZnO flower-like nanostructure sensor selective to ethanol in presence of CO and CH_4, Sensors and Actuators B: Chemical 169 (2012) 67–73.
[44] S.M. Chou I, L.G. Teoh, W.H. Lai, Y.H. Su, M.H. Hon, ZnO:Al thin film gas sensor for detection of ethanol vapor, Sensors 6 (2006) 1420–1427.
[45] C. Ge, C. Xie, S. Cai, Preparation and gas-sensing properties of Ce-doped ZnO thin-film sensors by dip-coating, Materials Science and Engineering B 137 (2007) 53–58.
[46] X. Cheng, H. Zhao, L. Huo, S. Gao, J. Zhao, ZnO nanoparticulate thin film: preparation, characterization and gas-sensing property, Sensors and Actuators B: Chemical 102 (2004) 248–252.
[47] Y. Zhang, J. Xu, Q. Xiang, H. Li, Q. Pan, P. Xu, Brush-like hierarchical ZnO nanostructures: synthesis, photoluminescence and gas sensor properties, Journal of Physical Chemistry C 113 (2009) 3430–3435.
[48] M.E. Franke, T.J. Koplin, U. Simon, Metal and metal oxide nanoparticles in chemiresistors: does the nanoscale matter? Small 2 (2006) 36–50.
[49] F. Pourfayaz, A. Khodadadi, Y. Mortazavi, S.S. Mohajerzadeh, CeO_2 doped SnO_2 sensor selective to ethanol in presence of CO, LPG and CH_4, Sensors and Actuators B: Chemical 108 (2005) 172–176.
[50] I. Kocemba, M. Wróbel-Jędrzejewska, A. Szychowska, J. Rynkowski, M. Główka, The properties of barium stannate and aluminum oxide-based gas sensor: the role of Al_2O_3 in this system, Sensors and Actuators B: Chemical 121 (2007) 401–405.

Biographies

Dr. Qing-Hong Xu is currently an assistant professor of Chemistry at State Key Laboratory of Chemical Resource Engineering, Beijing University of Chemical Technology, China. His research interests include inorganic/organic hybrids, inorganic synthesis etc.

Dong-Mei Xu is currently a third-year master student in Dr. Guo's group, in the College of Science, Beijing University of Chemical Technology, China. Her research interests focus on the preparation and characterization of gas sensing materials.

Mei-Yu Guan is currently a second-year master student in Dr. Guo's group, in the College of Science, Beijing University of Chemical Technology, China. Her research interests focus on the preparation and characterization of gas sensing materials.

Dr. Ying Guo is a Lecture at State Key Laboratory of Chemical Resource Engineering, Beijing University of Chemical Technology, China. Her work mainly focuses on the inorganic/organic nanocomposites for gas sensing application.

Dr. Qi Qi is a postdoctor in Professor Li's group at State Key Laboratory of Inorganic Synthesis & Preparative Chemistry, Jilin University, China. His research interests include studies of gas sensing mechanism of metal oxide materials.

Dr. Guo-Dong Li is a professor of State Key Laboratory of Inorganic Synthesis & Preparative Chemistry, Jilin University, China. His research interests focus on the preparation and characterization of porous materials and its application in host–guest materials as well as the synthesis of inorganic materials with novel function such as gas sensing materials, conductive materials etc.